

# On Efficient Language and Vision Assistants for Visually-Situated Natural Language Understanding: What Matters in Reading and Reasoning

**Geewook Kim**  
NAVER Cloud AI  
KAIST AI  
gwkim.rsrch@gmail.com

**Minjoon Seo**  
KAIST AI  
minjoon@kaist.ac.kr

## Abstract

Recent advancements in language and vision assistants have showcased impressive capabilities but suffer from a lack of transparency, limiting broader research and reproducibility. While open-source models handle general image tasks effectively, they face challenges with the high computational demands of complex visually-situated text understanding. Such tasks often require increased token inputs and large vision modules to harness high-resolution information. Striking a balance between model size and data importance remains an open question. This study aims to redefine the design of vision-language models by identifying key components and creating efficient models with constrained inference costs. By strategically formulating datasets, optimizing vision modules, and enhancing supervision techniques, we achieve significant improvements in inference throughput while maintaining high performance. Extensive experiments across models ranging from 160M to 13B parameters offer insights into model optimization. We will fully open-source our codebase, models, and datasets at <https://github.com/naver-ai/elva>.

## 1 Introduction

Recent advancements in integrating Large Language Models (LLMs) with computer vision have led to the creation of sophisticated Language-Vision Assistants. These systems are capable of interpreting text within images, enabling them to excel in complex tasks requiring both visual and textual understanding. Notably, models like GPT-4(V) (OpenAI, 2023) are able to leverage a single foundation model to handle various text-centric tasks. However, these models also face significant challenges related to transparency and accessibility, limiting broader utilization.

Open-source alternatives such as LLaVA (Liu et al., 2023c, 2024b) have emerged to address these

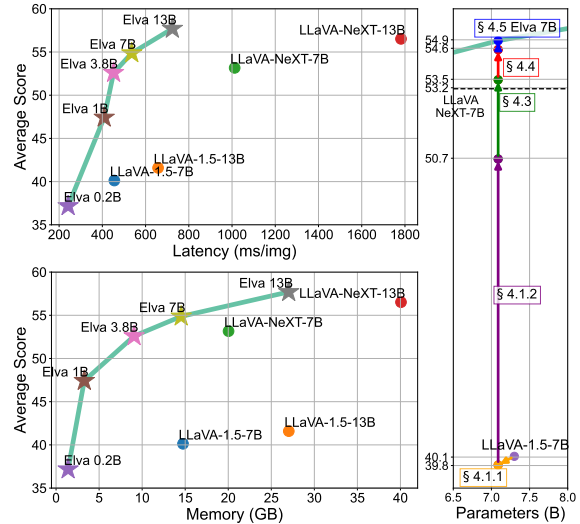


Figure 1: Graphical comparison illustrating average score against latency and memory consumption for various models. Scores are derived from eight benchmarks: DocVQA (Mathew et al., 2021), ChartQA (Masry et al., 2022), InfographicVQA (Mathew et al., 2022), SEED-IMG (Li et al., 2023), SEED-2-Plus (Li et al., 2024), MMStar (Chen et al., 2024), ScienceQA (Lu et al., 2022), and HallusionBench (Guan et al., 2024). See Section 4.2 for benchmark details. ELVA excels with high performance, reduced latency, and lower memory usage. Right: Performance improvements from LLaVA to ELVA, achieved through strategies in Section 4.

issues. However, as these models grow in complexity, concerns about their reproducibility and resource efficiency persist (Kim et al., 2023; Dong et al., 2024). Some open-source models provide only the model weights without comprehensive specifications, making replication and use more challenging.

In the fast-evolving realm of Vision-Language Models (VLMs), simply expanding model size and consuming more resources does not necessarily enhance practical utility. It is crucial to strike a balance between high performance and resource efficiency to democratize access to advanced VLMs.

Particularly, inference costs are a significant concern for practitioners developing real-world applications. Despite the importance of this balance, the fundamental elements that contribute to VLM success remain underexplored.

Traditionally, to enhance text comprehension, many VLMs increase their model resolution, often leading to larger and more resource-intensive models. In this work, we challenge this approach by introducing ELVA (Efficient Language and Vision Assistant), a suite of VLMs designed to maintain high performance while reducing inference costs and focusing on text-centric tasks. While we do increase training costs to a manageable extent, the primary research target of ELVA is to create models capable of handling high-resolution tasks with low inference costs.

Our key contributions are as follows:

1. **Efficiency and Reproducibility:** We present ELVA, an efficient and scalable model architecture trained on open-source data, demonstrating superior reproducibility and cost-effectiveness as shown in Figure 1.
2. **Empirical Validation:** We conduct thorough experiments to validate the effectiveness of ELVA’s primary components.
3. **Model Scalability:** We develop ELVA versions ranging from 0.2B to 13B parameters, showcasing its scalability and adaptability.
4. **Dataset Contributions:** To evaluate ELVA as a document assistant, we introduce two new datasets, CORD-Instruct and Parsing-Bench.
5. **Open-Source Initiative:** To foster further community research and ensure model reproducibility, we will open-source the trained models and datasets from this study.

Our ultimate goal is to shed light on the complexities of VLMs, helping readers identify the critical factors driving model success while presenting a practical, cost-effective solution with significant real-world applications. Following this introduction, §2 provides an overview of foundational LLaVA models; §3 discusses computational challenges; §4 outlines our proposed solutions; §5 presents our empirical results and analysis; §6 offers further analysis and ablations; and §7 along with §8 survey related works and conclude the study, respectively.

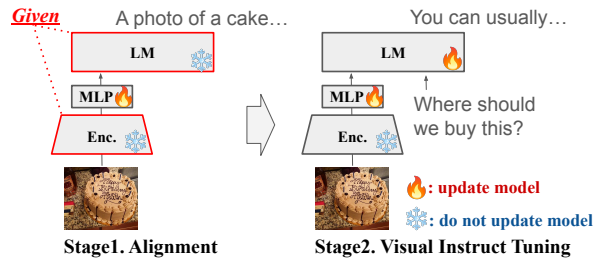


Figure 2: **Training pipeline** consists of two stages: alignment of visual and textual features through the MLP, followed by joint training of the LM and the MLP.

## 2 Large Language and Vision Assistants

**Architecture.** The LLaVA framework (Figure 2) employs a pre-trained Vision Transformer (ViT) as its vision encoder. Input images are resized and divided into patches of size  $n \times (p_h \times p_w \times c)$ , where  $n = (h/p_h) \times (w/p_w)$ . These patches are processed by the encoder to generate embeddings  $\{z_i \in \mathbb{R}^d\}$ , which are then adjusted using a multi-layer perceptron (MLP) for compatibility with the language model. The AnyRes mechanism (Liu et al., 2024b) allows processing of larger images by segmenting them into  $m$  parts. Each part is processed through the ViT, local embeddings are generated, and all are utilized. This ensures comprehensive understanding of varied image sizes and resolutions. However, this increases the total token count to  $n \times m$ , posing a computational challenge.

**Training Objectives and Datasets.** LLaVA is trained to minimize Cross-Entropy (CE) loss. During pre-training, it generates captions for images, with CE loss computed on the text. In the fine-tuning stage, given an image, question, and answer from the assistant, the loss is computed on the answer text. The LLaVA-1.5 dataset (Liu et al., 2023b) is widely used and this study aims to further enhance the dataset. More details are in Section 4.

## 3 Efficiency Challenges in LLaVA Models

This section addresses common overhead issues in LLaVA models, identifying critical limitations and defining the problem space for future work (Liu et al., 2024b; Dong et al., 2024).

### 3.1 Inference Overhead Sources

Inference overhead in LLaVA models stems from several factors:

- **Model Scale:** Larger models (e.g., 34B parameters) offer enhanced capabilities but incur significant computational costs.

Model	Token Usage (#tok)	s/img	Memory (GB)
LLaVA-1.5-7B	576	0.46	15
LLaVA-1.5-13B	576	0.66	27
LLaVA-NeXT-7B	approx. 1.7–2.9K	1.01	20
LLaVA-NeXT-13B	approx. 1.7–2.9K	1.78	40
LLaVA-NeXT-34B	approx. 1.7–2.9K	4.00	88

Table 1: Inference latency and memory costs for different LLaVA models. Tested with NVIDIA V100 GPUs.

- **Vision Encoder Complexity:** Advanced image encoders like SO400M and ViT-G (1.8B) improve performance but increase overhead (Sun et al., 2024; Zhai et al., 2023).
- **Image Resolution:** High resolutions (e.g., 900px) for detailed visual tasks like *DocVQA* (Mathew et al., 2021) increase computational demands on the vision encoder.
- **Vision Token Quantity:** Higher resolutions lead to more vision tokens, increasing the computational load on the LLM (e.g., LLaVA-NeXT uses up to 2880 tokens).

Higher image resolutions and complex tasks further increase the computational demands on vision encoders and language models.

### 3.2 Benchmarking Baseline Models

Resource usage during inference for LLaVA and LLaVA-NeXT models was evaluated on the *DocVQA* and *ChartQA* (Masry et al., 2022) test sets. As shown in Table 1, LLaVA-1.5 models showed manageable computational costs, operable on a single V100 GPU. However, LLaVA-NeXT models with up to 2.9K tokens presented significant challenges. Testing on an NVIDIA V100 32GB showed that LLaVA-NeXT-13/34B could not be accommodated on a single GPU. These findings emphasize the challenges of larger models, especially in resource-constrained environments.

### 3.3 Existing Approaches to Efficiency

Existing computationally demanding methods come with trade-offs. Sampler modules like the Perceiver resampler (Alayrac et al., 2022) reduce token count but are resource-intensive to train and may struggle with generating precise responses (Liu et al., 2024b). Separate models for detailed or concise responses complicate deployment (Bai et al., 2024; Laurençon et al., 2024).

Simpler approaches, such as those based on LLaVA (Liu et al., 2023c), are compatible with libraries like *SGLang* (Zheng et al., 2023b) and *transformers* (Wolf et al., 2020), facilitating broader use.

Improving these models for speed and performance remains a high-impact research area. For more on current trends, see Section 7.

## 4 Efficient Language and Vision Assistant

### 4.1 Preliminary: Base Architecture Modification and Initial Data Curation

To identify the most effective model architecture, we test various LLMs ranging from 160M to 13B as follows: Llama-160M, TinyVicuna-1B, Phi3-3.8B, Vicuna-7B, and Vicuna-13B.<sup>1</sup>

For the vision encoder, we replace the OpenAI CLIP-Large-336-14 module (LLaVA-1.5) with OpenAI CLIP-Base-224-32, using the Anyres technique to retain resolution while summarizing input into similar token count. OpenAI CLIP-Large-336-14 processes a 336x336 area into 576 tokens; OpenAI CLIP-Base-224-32 processes a 224x224 area into 49 tokens. Using Anyres, resolution is increased to 896x676px with a token count capped at 637, compared to LLaVA-NeXT’s 2880 tokens for 672x672px. However, this results in slight performance degradation (from LLaVA-1.5-7B’s 40.1 to 39.8; see §4.1.1 in Figure 1).

We then expand the dataset to enhance performance by incorporating data from LLaVAR (Zhang et al., 2023), Idefics2 (Laurençon et al., 2024), and several open-source datasets. This involves using 1.1 million samples for alignment tasks and 1 million samples for instruction tuning. Detailed dataset quantities are provided in the Appendix. As shown in Figure 1, this strategy is somewhat effective (39.8 to 50.7) but does not achieve the performance levels of LLaVA-NeXT-7B which reaches 53.2 (refer to §4.1.2 in Figure 1).

### 4.2 Problem Definition and Strategies

Despite multiple optimizations, the model displays performance issues, particularly generating hallucinations—incorrect responses due to inherent bias rather than accurate visual interpretation. These problems are evident in tasks requiring strong integration of visual and text information.

**Hypothesized Challenges.** We hypothesize two main challenges: (1) inadequate embeddings from

<sup>1</sup>Llama-160M: <https://huggingface.co/Felladrin/Llama-160M-Chat-v1>, TinyVicuna: <https://huggingface.co/Jiayi-Pan/Tiny-Vicuna-1B>, Phi3-3.8B (Abdin et al., 2024): <https://huggingface.co/microsoft/Phi-3-mini-4k-instruct>, Vicuna-7/13B (Zheng et al., 2023a): <https://huggingface.co/lmsys>

the vision encoder, and (2) poor understanding of basic text comprehension tasks, which is crucial for complex document interpretation.

**Improvement Strategies.** To address these challenges, we implement: (1) a more efficient vision encoder to enhance the quality of embeddings, and (2) a training regimen that prioritizes text comprehension before proceeding to more complex tasks.

To test our hypotheses, we conduct a series of comprehensive ablation experiments. Figure 1 illustrates our development stages. We track the effectiveness of our model modifications using various text-centric evaluation benchmarks, including DocVQA (**Doc**) (Mathew et al., 2021), ChartQA (**Chart**) (Masry et al., 2022), InfographicVQA (**Info**) (Mathew et al., 2022), and SEED-2-Plus (**SD2P**) (Li et al., 2024). Additionally, we employ widely-used general LVLMM benchmarks such as SEED-IMG (**SD-I**) (Li et al., 2023), MMStar (**MMS**) (Chen et al., 2024), ScienceQA-IMG (**SciQA**) (Lu et al., 2022), and HallusionBench (**Hall**) (Guan et al., 2024). Our primary objective is to enhance performance on text-focused tasks while maintaining competitive performance on general tasks and ensuring low inference costs.

In the followings, we introduce each proposed module in detail and conduct extensive ablation studies, analyzing the impact of removing each component from the final model configuration.

### 4.3 Developing an Enhanced Vision Encoder with Weight Averaging

To improve visually-situated NLU, we develop a new vision encoder optimized specifically for reading text within images. This encoder is designed to enhance resolution and computational efficiency while managing cost constraints.

Initially, we found that simply unfreezing the vision encoder while training the VLM (**C2**) does not yield significant improvements in performance. Next, we adopt a two-step approach. (1) We unfreeze the vision encoder and train it on a small VLM (1B scale) using text-centric datasets such as OCR-IDL (Biten et al., 2022). This training focuses on a "text reading task," where the model is tasked with reading text within images. This allows the vision encoder to adapt and enhance its text recognition capabilities. (2) We extract the enhanced vision encoder (*REncoder*) from this text-centric VLM. Notably, the text-centric VLM used for achieving *REncoder* is not utilized further in our

Vision Encoder Configuration	Text-Centric	General	Overall
<b>C1.</b> CLIP-B-224-AnyRes (CLIP)	40.3	54.5	47.4
<b>C2.</b> Unfreeze CLIP	34.1	47.6	40.9
<b>C3.</b> <i>REncoder</i> (RE)	45.2	52.2	48.7
<b>C4.</b> Avg (CLIP& RE)	45.6	54.4	50.0
<b>C5.</b> ELVA-encoder (Avg (CLIP& 12 REs))	45.7	54.7	50.2
<i>Supplementary ablations</i>			
<b>C6.</b> CLIP-L-336 (LLaVA-1.5 on our data)	37.5	58.6	48.1
<b>C7.</b> CLIP (7%) + <i>REncoder</i> (93%)	45.9	53.5	49.7

Table 2: Ablation Study Results for Different Vision Encoder Configurations. Average scores for text-centric tasks (DocVQA, ChartQA, InfoVQA, and SEED-2-Plus), and general image tasks (SEED, MMStar, ScienceQA, and HallusionBench) are reported. These results are obtained with Phi-3 (3.8B). The overall scores for other scales (from 1B to 13B) are shown in Figure 3.

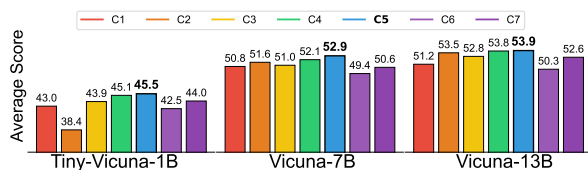


Figure 3: Performance of various vision encoder configurations at scales of 1B, 7B, and 13B. Average scores for each configuration (C1 to C7) across 8 benchmarks.

processes. When we train a VLM with the obtained *REncoder*, we observe significant improvements in text-centric tasks (**C3**), however, its performance on general image tasks still declines.

Now we have two expert encoders, the original CLIP for general tasks and the *REncoder*. Inspired by prior work, *Model soup* (Wortsman et al., 2022), we test with averaging the weights of the original encoder and the *REncoder*. Surprisingly, this method produces promising results (**C4**). Additionally, further adjusting the weight averaging ratios to lean more towards the *REncoder* provides marginally better text-centric performance (**C7**).

To further enhance robustness, we train 12 *REncoders* with different random seeds and then average their weights, a practice inspired by Wortsman et al. (2022). This averaging process, taking approximately 1.7 days on 8 V100 GPUs per phase, yields a vision encoder that substantially improves text comprehension while maintaining robust general capabilities (**C5**). The additional training details are in Appendix D.

In summary, the core idea is simple. We (1) **unfreeze the encoder and train a small VLM for text reading tasks, and retrieve the specialized encoder**, and (2) **make it robust to various tasks by applying weight averaging**. Finally, the produced vision encoder is used to build an efficient language and vision assistant, ELVA. Our new



**ELVA-encoder (C5)** brings substantial enhancements in text-centric tasks compared to the original base (C1). While there is still a reduction in general image performance compared to merely training LLaVA-1.5 on our data (C6), understanding the trade-offs in C6 is key to fully appreciating the balance we achieve. We effectively balance overall performance and computational cost within the scope of CLIP-Base parameters (88M). The ELVA-encoder configurations demonstrate notable success overall, as shown in Table 2 and Figure 3.

#### 4.4 Augmenting Text Understanding in Images with Read-and-Reason Prompts

We explore Visual Document Understanding (VDU) models utilizing pixel-based language modeling tasks, such as exhaustive image text reading during training (Kim et al., 2022; Lee et al., 2023). Models like LLaVA (Liu et al., 2023c,b) use OCR to preprocess images, augmenting user queries with OCR results. However, a comprehensive investigation of methods for supervising textual information during visual instruction tuning is lacking.

Table 3 shows ablation studies investigating text reading tasks during visual instruction tuning. Set **R1** follows standard practices using datasets without additional text reading components. In **R2**, inspired by prompting (Brown et al., 2020), we incorporate an initial QA task, "What is written in this image?" before QA on text-rich images. For example, with an image of a restaurant menu, the model first **reads all text before querying** about menu items or prices. This incremental addition improves performance significantly from **R1 to R2**, especially in text-rich tasks. We annotate datasets using OCR engines for this purpose.

Our further explorations assess this approach in resource-scarce environments, using 10% of the original instruction tuning dataset size. Figure 4 shows results across 1B to 13B parameter models. We also explore the supervision structure’s impact by comparing "Read and Reason" versus "Reason and Read" approaches. **R3** models perform text reading last to evaluate this. Results confirm that "Read and Reason" is more effective, emphasizing structured prompting’s importance in model learning. Lastly, we evaluate the effect of providing read text as context without explicit supervision (**R4**). Explicit supervision with text information yields marginal improvements in text-centric tasks.

In summary, the proposed core idea is to use RR-Prompt during model training to enhance text

	1B	3.8B	7B	13B
	Text/Gen/All	Text/Gen/All	Text/Gen/All	Text/Gen/All
<b>R1</b>	41.6/48.7/45.2	43.7/53.9/48.8	47.5/56.0/51.8	48.5/56.5/52.5
<b>R2</b>	42.4/48.6/45.5	45.7/54.7/50.2	49.2/56.6/52.9	50.4/57.4/53.9
<i>Supplementary ablations</i>				
<b>R3</b>	41.2/46.5/43.9	45.4/53.7/49.6	47.0/55.3/51.2	50.8/56.1/53.5
<b>R4</b>	42.0/48.8/45.4	44.1/54.2/49.1	48.2/56.0/52.1	49.6/57.6/53.6

Table 3: Comparison of different model sizes and RR-Prompt variants. **R1** represents standard models trained without additional text reading prompt. **R2** employs explicit initial text reading steps for text-rich tasks. **R3** carries out text reading at the end, while **R4** provides OCR results just as context without explicit supervision.

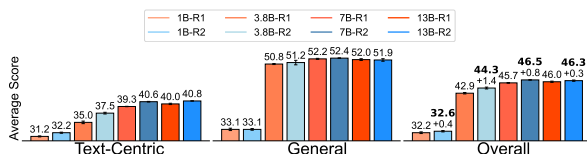


Figure 4: Using a 10% subset of the dataset, the impact of integrating the RR-Prompt during training is shown.

understanding in images. This approach, validated through ablation studies, shows significant performance improvements, especially in text-rich tasks. Note that the **RR-Prompt is used during training**; during inference, the model directly engages in reasoning, leveraging the enhanced capabilities acquired through the RR-Prompt, ensuring efficiency without needing an explicit text reading stage.

#### 4.5 Bringing It All Together

To develop a more robust model capable of handling a wider range of tasks, we scale up the model development by incorporating diverse datasets beyond merely text-centric tasks. Our final model integrates four additional datasets: Vision-Flan (Xu et al., 2024), RefCOCO (Kazemzadeh et al., 2014), VG (Krishna et al., 2017), and CORD (Park et al., 2019). By incorporating these additional datasets, we aim to enhance both the performance and generalizability of our model. The final training involved 11K steps with a batch size of 128. The specific dataset details and schedules are in the appendix. As demonstrated in Figure 1, our final configuration shows solid performance.

## 5 Experimental Assessment

In this section, we rigorously test and evaluate our ELVA models under varying conditions. We aim to understand their capabilities and limitations by benchmarking them against baseline models across

Model	# Param		#tok	s/img	vram	Text-Centric Benchmarks					General Multimodal Benchmarks						
	Vision	LM				Doc	Chart	Info	SD2P	PBen	SD-I	MMS	SciQA	Hall	AI2D	Math	LBen
LLaVA-v1-13B	300M	13B	576	1.43	26.9	9.8	7.0	19.9	39.5	14.0	51.2	32.9	62.4	43.0	43.9	25.9	69.9
LLaVA-1.5-7B	300M	7B	576	0.46	14.7	22.8	17.8	22.4	41.2	17.9	65.9	33.1	69.2	48.5	55.6	25.6	59.6
LLaVA-1.5-13B	300M	13B	576	0.66	27.0	24.5	18.5	24.9	44.4	19.6	68.2	34.1	72.3	45.7	60.7	27.7	66.1
LLaVA-NeXT-7B	300M	7B	1728-2880	1.01	20.0	68.3	51.9	31.6	51.7	49.6	69.8	38.2	69.0	44.8	66.8	31.8	<b>72.3</b>
LLaVA-NeXT-13B	300M	13B	1728-2880	1.78	40.1	<u>69.8</u>	59.0	<b>34.9</b>	<b>55.6</b>	<u>57.3</u>	<b>71.5</b>	<u>41.2</u>	73.4	46.7	71.7	34.1	<b>72.3</b>
<b>ELVA-0.2B (ours)</b>	88M	0.2B	98-637	0.24	1.4	44.7	50.3	14.8	31.4	12.3	37.8	31.5	39.0	48.1	31.0	27.0	28.4
<b>ELVA-1B (ours)</b>	88M	1B	98-637	0.41	3.3	62.6	57.7	23.7	36.8	27.3	52.3	32.6	63.3	50.4	46.9	31.7	36.0
<b>ELVA-3.8B (ours)</b>	88M	3.8B	98-637	0.45	9.1	66.5	<u>62.5</u>	24.3	43.4	24.4	61.1	35.9	73.4	53.7	64.2	34.9	40.7
<b>ELVA-7B (ours)</b>	88M	7B	98-637	0.54	14.5	69.1	61.8	30.7	47.7	45.0	62.6	35.4	74.7	<b>56.8</b>	66.2	<u>36.6</u>	50.7
<b>ELVA-13B (ours)</b>	88M	13B	98-637	0.72	27.0	<b>71.7</b>	<b>65.2</b>	<u>34.6</u>	<u>52.6</u>	<b>59.2</b>	65.3	37.9	<u>77.7</u>	<b>56.8</b>	<b>69.3</b>	<b>38.1</b>	51.0
<i>Supplementary baselines</i>																	
QwenVL-7B	1882M	7B	224	0.50	19.2	65.1	60.2	-	41.0	-	56.5	33.9	60.6	37.4	57.2	15.5	12.9
QwenVL-7B-Chat	1882M	7B	224	0.56	19.2	62.6	49.3	-	46.9	-	62.9	34.0	64.0	40.8	59.7	34.9	67.7
PaliGemma-3B	428M	3B	1024	0.98	10.3	-	33.8	-	49.8	-	<u>70.0</u>	<b>48.6</b>	<b>94.3</b>	53.0	<b>69.3</b>	28.7	36.9

Table 4: **Performance Comparison Across Different Models and Benchmarks.** This table summarizes model sizes (Vision and LM), token counts (#tok), latency (s/img), and memory cost (vram). The performance metrics across various benchmarks are presented, showcasing each model’s strengths and weaknesses in different challenges.

both text-based and image-based tasks.

## 5.1 Framework

Our evaluation process extends beyond our initial eight datasets, utilized in our ablation studies (See §4.2). To further enrich our examination, we have included additional diverse datasets such as **AI2D** (Kembhavi et al., 2016), MathVista-TestMini (Lu et al., 2024) (**Math**), LLaVA-Bench (Liu et al., 2023c) (**LBen**), along with Parsing-Bench (**PBen**) proposed in this work.

## 5.2 Generated Scenario-Based Benchmarks

In our research, we identify a significant gap in datasets representing real-world user scenarios for document assistants. To address this, we create the following datasets. These datasets will be open-source, and more details are in the appendix:

**CORD-Instruct.** Building on the CORD dataset, which consists of Indonesian receipts and their JSON annotations, CORD-Instruct provides instructional sets for models to generate outputs in JSON, XML, or Markdown formats. We utilize the OpenAI GPT-3.5 API to create these instructional sets, ensuring the exclusion of any erratic samples.

**Parsing-Bench.** Inspired by the LLaVA-Bench and LLM-as-a-Judge (Zheng et al., 2023a), we develop PARSING-BENCH to address the limitations of existing benchmarks like LLaVA-Bench, which include limited document-related samples and do not sufficiently reflect real user needs. Figure 6 presents example cases and model predictions. To

test the model’s ability to extract information from new documents, we create this dataset using 30 images from Brazilian Identity Documents (Álysson Soares et al., 2020) and SROIE (Huang et al., 2019), which are not used during training.

## 5.3 Results

Table 4 presents a detailed comparison of our ELVA models against baselines like PaliGemma (Beyer et al., 2022), QwenVL (Bai et al., 2024), and LLaVA across various benchmarks and tasks. The results, either reproduced or sourced from original papers, have been validated using VLMEvalKit (Contributors, 2023) and the official code by Liu et al. (2023c).

The ELVA models consistently demonstrate strong performance in text-centric and general image benchmarks. The ELVA-0.2B model, despite its smaller parameter count, performs admirably across various tasks. Larger models like ELVA-1B, ELVA-3.8B, and ELVA-7B exhibit superior performance, showcasing the benefits of increased model capacity. Notably, ELVA-7B strikes a fine balance between size and effectiveness. Our largest model, ELVA-13B, achieves top scores in benchmarks such as Doc, Chart, Hall, AI2D, Math, and PBen, underscoring the efficacy of scaling model capacity for vision-and-language tasks. Additionally, ELVA-13B remains efficient in terms of latency, reinforcing its practicality for diverse applications.

A notable limitation is observed in the LLaVA-Bench, where ELVA models underperform compared to the LLaVA series. Given this dataset only

Method	s/img	vram	Doc	Chart	Info	SD2P
LLaVA-NeXT-7B	1.01	20.0	68.3	51.9	31.6	51.7
– w/ max. 1728 tokens	0.70	17.1	51.7	48.0	27.9	44.9
<b>ELVA-7B (ours)</b>	<b>0.54</b>	<b>14.5</b>	<b>69.1</b>	<b>61.8</b>	<b>30.7</b>	<b>47.7</b>
LLaVA-NeXT-13B	1.78	40.1	69.8	59.0	34.9	55.6
– w/ max. 1728 tokens	1.11	30.4	53.9	52.3	30.9	49.2
<b>ELVA-13B (ours)</b>	<b>0.72</b>	<b>27.0</b>	<b>71.7</b>	<b>65.2</b>	<b>34.6</b>	<b>52.6</b>

Table 5: Ablations on reduced vision token counts.

comprises 24 images, interpretation requires caution. Detailed analysis will be provided in §6.3.

In summary, ELVA models deliver robust performance across a wide range of tasks and benchmarks. While increased model capacity generally enhances performance, efficiency and latency considerations are crucial for practical deployment. Our results underscore ELVA’s proficiency in efficiently addressing diverse vision-and-language challenges, providing valuable insights into their performance and reliability across various contexts.

## 6 Further Analyses and Discussions

### 6.1 Ablations with LLaVA-NeXT Variants

To test the impact of reducing the number of tokens in LLaVA-NeXT models, we constrain the grid size, resulting in a maximum token count of 1728 (either 336x672 or 672x336 pixels). This adjustment speeds up processing while allowing us to evaluate performance changes across benchmarks. As shown in Table 5, reducing the vision token count leads to significant performance drops across all evaluated tasks. For example, the performance of the 13B model on DocVQA decreases from 69.8 to 53.9 when the token count is restricted, with similar trends observed in other variants.

In contrast, ELVA models demonstrate strong performance along with improved efficiency in both speed and memory usage, underlining their robustness in handling vision-and-language tasks efficiently. This analysis highlights the trade-off between token count and model performance: while reducing tokens can enhance computational efficiency, it may lead to a compromise in accuracy. The ELVA models effectively balance performance and efficiency, outperforming larger LLaVA-NeXT configurations even with reduced token counts.

### 6.2 Discussion on Memory and Time Costs

We evaluate latency in seconds per sample for benchmarks like ChartQA and DocVQA, as these tasks relate closely to real-world document information extraction scenarios. Multiple-choice eval-

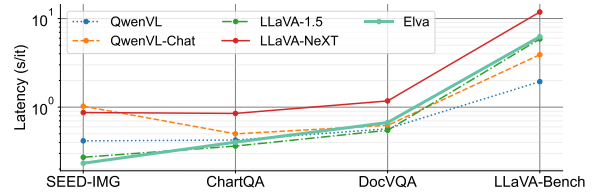


Figure 5: Latency comparison across multiple datasets.

uations like SD-I are less indicative of actual user scenarios, complicating meaningful latency comparisons. Task-oriented benchmarks like DocVQA offer more user-centric metrics. Benchmarks requiring longer answers, such as LLaVA-Bench, show inconsistent results due to varied answer lengths across models. Consequently, we focus on ChartQA and DocVQA for latency assessments but also include SD-I and LLaVA-Bench results in Figure 5. These findings indicate ELVA maintains commendable latency across varied contexts.

While this study primarily focuses on inference time costs, training costs are equally important for practitioners. Despite processing a substantial dataset, our lightweight vision encoding facilitates high training sample throughput. Our training time costs are approximately 1.38 to 1.8 times that of LLaVA-NeXT, representing a reasonable trade-off given the efficiency and performance gains. Our approach remains competitive and more resource-efficient compared to several contemporary models. For detailed analysis, please refer to Appendix A.

Regarding memory usage, practical deployment often uses 4-bit quantization (Dettmers et al., 2023), significantly reducing memory costs. For example, the LLaVA-NeXT-13B model originally requires two V100 GPUs but can run on a single V100 with quantization, though with increased latency and performance degradation. Despite limitations, quantization is promising and likely to improve with advancements. Our ELVA models, designed for efficiency, complement these advancements, promising even greater value when combined with quantization techniques. Future work will likely enhance these models’ efficacy in deployment.

### 6.3 Case Study on LLM-as-a-Judge Sets

ELVA models perform robustly across benchmarks, excelling in text-centric tasks, but show performance dips on LLaVA-Bench. These issues often stem from failures in entity recognition, resulting in logically correct but penalized responses. For example, when asked to name an anime charac-

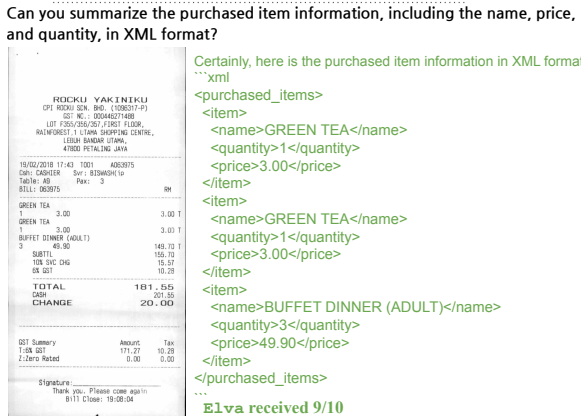
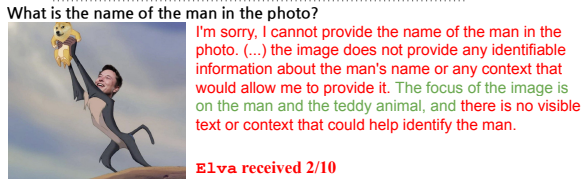
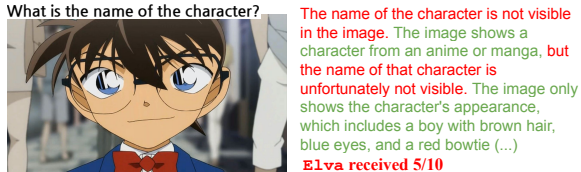


Figure 6: Results on LLaVA-Bench and Parsing-Bench.

ter, ELVA scores 5/10 for failing to provide the correct name despite a detailed description. Similarly, it scores only 2/10 in identifying a person in a photo without textual clues. These dips highlight limitations in the ELVA-encoder’s (88M) entity memorization capacity and the lack of contextual data within images. Adding targeted data during instruct-tuning might address these issues, though feasibility is debatable. On the other hands, ELVA excels in information comprehension tasks, such as summarizing receipt data into XML format, scoring 9/10. This shows its ability to accurately read, comprehend, and organize text information. While ELVA is efficient, it remains competitive to other models rather than significantly superior. Future research may focus on enhancing the vision encoder and improving contextual understanding to overcome these limitations.

## 6.4 Discussion on Leveraging OCR

Incorporating OCR can be effective for handling text-rich high-resolution images. For instance, Kim et al. (2023) utilize OCR in their VLM for VDU tasks, suggesting its potential for models like LLaVA or ELVA. When OCR outputs are incorporated as contextual information during inference, as demonstrated in Table 6, notable enhancements

Method	Doc	Chart	Info	SD2P
LLaVA-NeXT-7B	74.5 (↑6.2)	53.7 (↑1.8)	35.5 (↑3.9)	55.3 (↑3.6)
<b>ELVA-7B (ours)</b>	<b>77.8 (↑8.7)</b>	<b>64.0 (↑2.2)</b>	<b>39.5 (↑8.8)</b>	<b>55.7 (↑8.0)</b>
LLaVA-NeXT-13B	76.5 (↑6.7)	62.5 (↑3.5)	40.4 (↑5.5)	58.9 (↑3.3)
<b>ELVA-13B (ours)</b>	<b>81.1 (↑9.4)</b>	<b>67.5 (↑2.3)</b>	<b>44.8 (↑10.2)</b>	<b>60.6 (↑8.0)</b>

Table 6: Performance improvement with OCR.

are observed, particularly benefiting ELVA. However, OCR processing has costs. Using the CLOVA OCR API<sup>2</sup>, our tests on the DocVQA dataset average about 4 seconds per sample. Faster OCR engines exist but often at the expense of accuracy. Additionally, upscaling VLMs to handle very high resolutions (e.g., 4K, 8K) may not be practical. Thus, leveraging OCR and similar tools remains a valuable area of exploration, aiming to balance specialized tools and VLMs for optimal performance.

## 7 Related Work

Visually-Situated NLU has evolved significantly, starting with heavy reliance on OCR for text extraction. A major advancement was marked by Xu et al. (2020), integrating textual and layout information for sophisticated document understanding. The field progressed to OCR-free models (Kim et al., 2022; Lee et al., 2023), enhancing flexibility and accuracy. Further, LLMs aim to jointly process visual and textual data, enhancing cross-modal understanding. LLaVA (Liu et al., 2023c) demonstrate efficient cross-modal performance. In VDU, Kim et al. (2023) use a hybrid approach, balancing OCR-free and OCR-dependent modes. More recently, high-resolution processing is central to models (Liu et al., 2024b; Dong et al., 2024), which achieve superior results despite computational demands. For additional comparisons with recent models, refer to Appendix A.

## 8 Conclusion

This study introduces ELVA, a robust and efficient model framework excelling in text-centric and visual tasks. Our empirical studies show ELVA models consistently outperform existing baselines, achieving notable efficiency in memory usage and latency. Challenges in entity recognition and contextual understanding highlight areas for improvement. Future research should focus on refining these aspects to enhance ELVA’s performance and robustness, ultimately solidifying its position as a leading solution in visually-situated NLU.

<sup>2</sup><https://clova.ai/ocr/en>



## 9 Limitations

Despite the significant advancements demonstrated by ELVA, several limitations remain. Firstly, ELVA occasionally struggles with recognizing specific entities and fully understanding contextual nuances within images, leading to penalized responses despite logical accuracy. That is, while ELVA excels in text-centric tasks, it might have limitations in the vision encoder’s ability to memorize entities and handle contextual data.

Incorporating OCR is beneficial for processing text-rich, high-resolution images, but it introduces latency and potential accuracy trade-offs. Moreover, managing very high-resolution images (4K or 8K) still remains challenging due to the balance required between performance improvements and computational resources.

While ELVA achieves lower inference costs and maintains a reasonable training time, the substantial data volume processed can lead to moderate time differences, as discussed in Appendix A. This underscores the importance of continued optimization in both training efficiency and performance.

Future research should focus on refining entity recognition, contextual understanding, training efficiency, and OCR handling. Investigating the balance between specialized tools like OCR and the core VLM is essential for optimizing performance. Additionally, expanding ELVA’s capabilities to handle multilingual tasks will further increase its applicability and utility.

## 10 Ethical Considerations

Developing ELVA involves important ethical responsibilities such as reducing data biases and ensuring transparency. To manage these, we use only controlled and verified open-source datasets for model training. Currently, we rely on the autoregressive models’ direct output, but we could also use post-processing techniques or additional training methods to address biases and privacy issues better. By open-sourcing our models and datasets, we encourage peer reviews and collaboration to solve ethical challenges, promoting accountability. These steps help ensure that ELVA upholds high ethical standards and is used for beneficial purposes while minimizing risks.

## Acknowledgements

We extend our sincere gratitude to Bado Lee, Daehee Kim, Taeho Kil, and Hodong Lee for their

meticulous proofreading of this manuscript. Their input greatly increased its clarity and coherence. We are also immensely grateful to our colleagues in the NAVER Cloud Hyperscale AI Vision Understanding Team and KAIST AI LKLab. Their constant support and encouragement have been a great source of motivation throughout this work.

## References

- Marah Abdin, Sam Ade Jacobs, Ammar Ahmad Awan, Jyoti Aneja, Ahmed Awadallah, Hany Awadalla, Nguyen Bach, Amit Bahree, Arash Bakhtiari, Jianmin Bao, Harkirat Behl, Alon Benhaim, Misha Bilenko, Johan Bjorck, Sébastien Bubeck, Qin Cai, Martin Cai, Caio César Teodoro Mendes, Weizhu Chen, Vishrav Chaudhary, Dong Chen, Dongdong Chen, Yen-Chun Chen, Yi-Ling Chen, Parul Chopra, Xiyang Dai, Allie Del Giorno, Gustavo de Rosa, Matthew Dixon, Ronen Eldan, Victor Fragoso, Dan Iter, Mei Gao, Min Gao, Jianfeng Gao, Amit Garg, Abhishek Goswami, Suriya Gunasekar, Emman Haider, Junheng Hao, Russell J. Hewett, Jamie Huynh, Mojan Javaheripi, Xin Jin, Piero Kauffmann, Nikos Karampatziakis, Dongwoo Kim, Mahoud Khademi, Lev Kurilenko, James R. Lee, Yin Tat Lee, Yuanzhi Li, Yunsheng Li, Chen Liang, Lars Liden, Ce Liu, Mengchen Liu, Weishung Liu, Eric Lin, Zeqi Lin, Chong Luo, Piyush Madan, Matt Mazzola, Arindam Mitra, Hardik Modi, Anh Nguyen, Brandon Norick, Barun Patra, Daniel Perez-Becker, Thomas Portet, Reid Pryzant, Heyang Qin, Marko Radmilac, Corby Rosset, Sambudha Roy, Olatunji Ruwase, Olli Saarikivi, Amin Saied, Adil Salim, Michael Santacroce, Shital Shah, Ning Shang, Hiteshi Sharma, Swadheen Shukla, Xia Song, Masahiro Tanaka, Andrea Tupini, Xin Wang, Lijuan Wang, Chunyu Wang, Yu Wang, Rachel Ward, Guanhua Wang, Philipp Witte, Haiping Wu, Michael Wyatt, Bin Xiao, Can Xu, Jiahang Xu, Weijian Xu, Sonali Yadav, Fan Yang, Jianwei Yang, Ziyi Yang, Yifan Yang, Donghan Yu, Lu Yuan, Chengruidong Zhang, Cyril Zhang, Jianwen Zhang, Li Lyna Zhang, Yi Zhang, Yue Zhang, Yunan Zhang, and Xiren Zhou. 2024. [Phi-3 technical report: A highly capable language model locally on your phone](#). *Preprint*, arXiv:2404.14219.
- Jean-Baptiste Alayrac, Jeff Donahue, Pauline Luc, Antoine Miech, Iain Barr, Yana Hasson, Karel Lenc, Arthur Mensch, Katherine Millican, Malcolm Reynolds, Roman Ring, Eliza Rutherford, Serkan Cabi, Tengda Han, Zhitao Gong, Sina Samangooei, Marianne Monteiro, Jacob Menick, Sebastian Borgeaud, Andrew Brock, Aida Nematzadeh, Saahand Sharifzadeh, Mikolaj Binkowski, Ricardo Barreira, Oriol Vinyals, Andrew Zisserman, and Karen Simonyan. 2022. [Flamingo: a visual language model for few-shot learning](#). In *Advances in Neural Information Processing Systems*.
- Jinze Bai, Shuai Bai, Shusheng Yang, Shijie Wang, Sinan Tan, Peng Wang, Junyang Lin, Chang Zhou,

- and Jingren Zhou. 2024. [Qwen-VL: A versatile vision-language model for understanding, localization, text reading, and beyond](#).
- Lucas Beyer, Xiaohua Zhai, and Alexander Kolesnikov. 2022. Big vision. [https://github.com/google-research/big\\_vision](https://github.com/google-research/big_vision).
- Ali Furkan Biten, Ruben Tito, Lluís Gomez, Ernest Valveny, and Dimosthenis Karatzas. 2022. Ocr-idl: Ocr annotations for industry document library dataset. *arXiv preprint arXiv:2202.12985*.
- Tom Brown, Benjamin Mann, Nick Ryder, Melanie Subbiah, Jared D Kaplan, Prafulla Dhariwal, Arvind Neelakantan, Pranav Shyam, Girish Sastry, Amanda Askell, Sandhini Agarwal, Ariel Herbert-Voss, Gretchen Krueger, Tom Henighan, Rewon Child, Aditya Ramesh, Daniel Ziegler, Jeffrey Wu, Clemens Winter, Chris Hesse, Mark Chen, Eric Sigler, Mateusz Litwin, Scott Gray, Benjamin Chess, Jack Clark, Christopher Berner, Sam McCandlish, Alec Radford, Ilya Sutskever, and Dario Amodei. 2020. Language models are few-shot learners. In *Advances in Neural Information Processing Systems*, volume 33, pages 1877–1901. Curran Associates, Inc.
- Keqin Chen, Zhao Zhang, Weili Zeng, Richong Zhang, Feng Zhu, and Rui Zhao. 2023a. Shikra: Unleashing multimodal llm’s referential dialogue magic. *arXiv preprint arXiv:2306.15195*.
- Lin Chen, Jinsong Li, Xiaoyi Dong, Pan Zhang, Yuhang Zang, Zehui Chen, Haodong Duan, Jiaqi Wang, Yu Qiao, Dahua Lin, et al. 2024. Are we on the right way for evaluating large vision-language models? *arXiv preprint arXiv:2403.20330*.
- Lin Chen, Jisong Li, Xiaoyi Dong, Pan Zhang, Conghui He, Jiaqi Wang, Feng Zhao, and Dahua Lin. 2023b. Sharegpt4v: Improving large multimodal models with better captions. *arXiv preprint arXiv:2311.12793*.
- Xiangxiang Chu, Limeng Qiao, Xinyu Zhang, Shuang Xu, Fei Wei, Yang Yang, Xiaofei Sun, Yiming Hu, Xinyang Lin, Bo Zhang, and Chunhua Shen. 2024. [Mobilevlm v2: Faster and stronger baseline for vision language model](#). *Preprint*, arXiv:2402.03766.
- OpenCompass Contributors. 2023. Opencompass: A universal evaluation platform for foundation models. <https://github.com/open-compass/opencompass>.
- Wenliang Dai, Junnan Li, Dongxu Li, Anthony Tiong, Junqi Zhao, Weisheng Wang, Boyang Li, Pascale Fung, and Steven Hoi. 2023. [InstructBLIP: Towards general-purpose vision-language models with instruction tuning](#). In *Thirty-seventh Conference on Neural Information Processing Systems*.
- Tim Dettmers, Artidoro Pagnoni, Ari Holtzman, and Luke Zettlemoyer. 2023. [QLoRA: Efficient finetuning of quantized LLMs](#). In *Thirty-seventh Conference on Neural Information Processing Systems*.
- Xiaoyi Dong, Pan Zhang, Yuhang Zang, Yuhang Cao, Bin Wang, Linke Ouyang, Songyang Zhang, Haodong Duan, Wenwei Zhang, Yining Li, Hang Yan, Yang Gao, Zhe Chen, Xinyue Zhang, Wei Li, Jingwen Li, Wenhai Wang, Kai Chen, Conghui He, Xingcheng Zhang, Jifeng Dai, Yu Qiao, Dahua Lin, and Jiaqi Wang. 2024. Internlm-xcomposer2-4khd: A pioneering large vision-language model handling resolutions from 336 pixels to 4k hd. *arXiv preprint arXiv:2404.06512*.
- Tianrui Guan, Fuxiao Liu, Xiyang Wu, Ruiqi Xian, Zongxia Li, Xiaoyu Liu, Xijun Wang, Lichang Chen, Furong Huang, Yaser Yacoob, Dinesh Manocha, and Tianyi Zhou. 2024. Hallusionbench: An advanced diagnostic suite for entangled language hallucination and visual illusion in large vision-language models. In *Proceedings of the IEEE/CVF Conference on Computer Vision and Pattern Recognition (CVPR)*, pages 14375–14385.
- Yu-Chung Hsiao, Fedir Zubach, Maria Wang, and Jindong Chen. 2024. [Screenqa: Large-scale question-answer pairs over mobile app screenshots](#). *Preprint*, arXiv:2209.08199.
- Anwen Hu, Haiyang Xu, Jiabo Ye, Ming Yan, Liang Zhang, Bo Zhang, Chen Li, Ji Zhang, Qin Jin, Fei Huang, and Jingren Zhou. 2024. [mplug-docowl 1.5: Unified structure learning for ocr-free document understanding](#). *Preprint*, arXiv:2403.12895.
- Zheng Huang, Kai Chen, Jianhua He, Xiang Bai, Dimosthenis Karatzas, Shijian Lu, and C. V. Jawahar. 2019. [Icdar2019 competition on scanned receipt ocr and information extraction](#). In *2019 International Conference on Document Analysis and Recognition (ICDAR)*, pages 1516–1520.
- Kushal Kafle, Scott Cohen, Brian Price, and Christopher Kanan. 2018. Dvqa: Understanding data visualizations via question answering. In *CVPR*.
- Sahar Kazemzadeh, Vicente Ordonez, Mark Matten, and Tamara Berg. 2014. [ReferItGame: Referring to objects in photographs of natural scenes](#). In *Proceedings of the 2014 Conference on Empirical Methods in Natural Language Processing (EMNLP)*, pages 787–798, Doha, Qatar. Association for Computational Linguistics.
- Aniruddha Kembhavi, Michael Salvato, Eric Kolve, Minjoon Seo, Hannaneh Hajishirzi, and Ali Farhadi. 2016. [A diagram is worth a dozen images](#). *ArXiv*, abs/1603.07396.
- Geewook Kim, Teakgyu Hong, Moonbin Yim, Jeongyeon Nam, Jinyoung Park, Jinyeong Yim, Wonseok Hwang, Sangdoon Yun, Dongyoon Han, and Seunghyun Park. 2022. [OCR-Free Document Understanding Transformer](#). In *Computer Vision – ECCV 2022*, pages 498–517, Cham. Springer Nature Switzerland.
- Geewook Kim, Hodong Lee, Daehee Kim, Haeji Jung, Sanghee Park, Yoonsik Kim, Sangdoon Yun, Taeho

- Kil, Bado Lee, and Seunghyun Park. 2023. [Visually-situated natural language understanding with contrastive reading model and frozen large language models](#). In *Proceedings of the 2023 Conference on Empirical Methods in Natural Language Processing*, pages 11989–12010, Singapore. Association for Computational Linguistics.
- Ranjay Krishna, Yuke Zhu, Oliver Groth, Justin Johnson, Kenji Hata, Joshua Kravitz, Stephanie Chen, Yannis Kalantidis, Li-Jia Li, David A. Shamma, Michael S. Bernstein, and Li Fei-Fei. 2017. [Visual genome: Connecting language and vision using crowdsourced dense image annotations](#). *Int. J. Comput. Vis.*, 123(1):32–73.
- Hugo Laurençon, Léo Tronchon, Matthieu Cord, and Victor Sanh. 2024. [What matters when building vision-language models?](#) *Preprint*, arXiv:2405.02246.
- Kenton Lee, Mandar Joshi, Iulia Raluca Turc, Hexiang Hu, Fangyu Liu, Julian Martin Eisenschlos, Urvashi Khandelwal, Peter Shaw, Ming-Wei Chang, and Kristina Toutanova. 2023. [Pix2Struct: Screenshot parsing as pretraining for visual language understanding](#). In *Proceedings of the 40th International Conference on Machine Learning*, volume 202 of *Proceedings of Machine Learning Research*, pages 18893–18912. PMLR.
- Bohao Li, Yuying Ge, Yi Chen, Yixiao Ge, Ruimao Zhang, and Ying Shan. 2024. [Seed-bench-2-plus: Benchmarking multimodal large language models with text-rich visual comprehension](#). *arXiv preprint arXiv:2404.16790*.
- Bohao Li, Rui Wang, Guangzhi Wang, Yuying Ge, Yixiao Ge, and Ying Shan. 2023. [Seed-bench: Benchmarking multimodal llms with generative comprehension](#). *arXiv preprint arXiv:2307.16125*.
- Fuxiao Liu, Kevin Lin, Linjie Li, Jianfeng Wang, Yaser Yacoob, and Lijuan Wang. 2023a. [Aligning large multi-modal model with robust instruction tuning](#). *arXiv preprint arXiv:2306.14565*.
- Fuxiao Liu, Xiaoyang Wang, Wenlin Yao, Jianshu Chen, Kaiqiang Song, Sangwoo Cho, Yaser Yacoob, and Dong Yu. 2024a. [MMC: Advancing multimodal chart understanding with large-scale instruction tuning](#). In *Proceedings of the 2024 Conference of the North American Chapter of the Association for Computational Linguistics: Human Language Technologies (Volume 1: Long Papers)*, pages 1287–1310, Mexico City, Mexico. Association for Computational Linguistics.
- Haotian Liu, Chunyuan Li, Yuheng Li, and Yong Jae Lee. 2023b. [Improved baselines with visual instruction tuning](#).
- Haotian Liu, Chunyuan Li, Yuheng Li, Bo Li, Yuanhan Zhang, Sheng Shen, and Yong Jae Lee. 2024b. [Llava-next: Improved reasoning, ocr, and world knowledge](#).
- Haotian Liu, Chunyuan Li, Qingyang Wu, and Yong Jae Lee. 2023c. [Visual instruction tuning](#).
- Pan Lu, Hritik Bansal, Tony Xia, Jiacheng Liu, Chunyuan Li, Hannaneh Hajishirzi, Hao Cheng, Kai-Wei Chang, Michel Galley, and Jianfeng Gao. 2024. [Mathvista: Evaluating mathematical reasoning of foundation models in visual contexts](#). In *International Conference on Learning Representations (ICLR)*.
- Pan Lu, Swaroop Mishra, Tony Xia, Liang Qiu, Kai-Wei Chang, Song-Chun Zhu, Oyvind Taffjord, Peter Clark, and Ashwin Kalyan. 2022. [Learn to explain: Multimodal reasoning via thought chains for science question answering](#). In *The 36th Conference on Neural Information Processing Systems (NeurIPS)*.
- Ahmed Masry, Xuan Long Do, Jia Qing Tan, Shafiq Joty, and Enamul Hoque. 2022. [ChartQA: A benchmark for question answering about charts with visual and logical reasoning](#). In *Findings of the Association for Computational Linguistics: ACL 2022*, pages 2263–2279, Dublin, Ireland. Association for Computational Linguistics.
- Minesh Mathew, Viraj Bagal, Rubèn Tito, Dimosthenis Karatzas, Ernest Valveny, and C.V. Jawahar. 2022. [InfographicVQA](#). In *Proceedings of the IEEE/CVF Winter Conference on Applications of Computer Vision (WACV)*, pages 1697–1706.
- Minesh Mathew, Dimosthenis Karatzas, and CV Jawahar. 2021. [Docvqa: A dataset for vqa on document images](#). In *Proceedings of the IEEE/CVF winter conference on applications of computer vision*, pages 2200–2209.
- OpenAI. 2023. [GPT-4 Technical Report](#). *Preprint*, arXiv:2303.08774.
- Seunghyun Park, Seung Shin, Bado Lee, Junyeop Lee, Jaeheung Surh, Minjoon Seo, and Hwalsuk Lee. 2019. [Cord: A consolidated receipt dataset for post-ocr parsing](#). In *Document Intelligence Workshop at Neural Information Processing Systems*.
- Quan Sun, Jinsheng Wang, Qiying Yu, Yufeng Cui, Fan Zhang, Xiaosong Zhang, and Xinlong Wang. 2024. [Eva-clip-18b: Scaling clip to 18 billion parameters](#). *Preprint*, arXiv:2402.04252.
- Ryota Tanaka, Kyosuke Nishida, and Sen Yoshida. 2021. [VisualMRC: Machine Reading Comprehension on Document Images](#). In *Thirty-Fifth AAAI Conference on Artificial Intelligence, AAAI 2021, Thirty-Third Conference on Innovative Applications of Artificial Intelligence, IAAI 2021, The Eleventh Symposium on Educational Advances in Artificial Intelligence, EAAI 2021, Virtual Event, February 2-9, 2021*, pages 13878–13888. AAAI Press.
- Thomas Wolf, Lysandre Debut, Victor Sanh, Julien Chaumond, Clement Delangue, Anthony Moi, Pierric Cistac, Tim Rault, Remi Louf, Morgan Funtowicz, Joe Davison, Sam Shleifer, Patrick von Platen,



- Clara Ma, Yacine Jernite, Julien Plu, Canwen Xu, Teven Le Scao, Sylvain Gugger, Mariama Drame, Quentin Lhoest, and Alexander Rush. 2020. [Trans-formers: State-of-the-art natural language processing](#). In *Proceedings of the 2020 Conference on Empirical Methods in Natural Language Processing: System Demonstrations*, pages 38–45, Online. Association for Computational Linguistics.
- Mitchell Wortsman, Gabriel Ilharco, Samir Ya Gadre, Rebecca Roelofs, Raphael Gontijo-Lopes, Ari S Morcos, Hongseok Namkoong, Ali Farhadi, Yair Carmon, Simon Kornblith, and Ludwig Schmidt. 2022. [Model soups: averaging weights of multiple fine-tuned models improves accuracy without increasing inference time](#). In *Proceedings of the 39th International Conference on Machine Learning*, volume 162 of *Proceedings of Machine Learning Research*, pages 23965–23998. PMLR.
- Yiheng Xu, Minghao Li, Lei Cui, Shaohan Huang, Furu Wei, and Ming Zhou. 2020. [LayoutLM: Pre-training of Text and Layout for Document Image Understanding](#). In *KDD '20: The 26th ACM SIGKDD Conference on Knowledge Discovery and Data Mining, Virtual Event, CA, USA, August 23-27, 2020*, pages 1192–1200. ACM.
- Zhiyang Xu, Chao Feng, Rulin Shao, Trevor Ashby, Ying Shen, Di Jin, Yu Cheng, Qifan Wang, and Lifu Huang. 2024. [Vision-flan: Scaling human-labeled tasks in visual instruction tuning](#). *arXiv preprint arXiv:2402.11690*.
- Xiaohua Zhai, Basil Mustafa, Alexander Kolesnikov, and Lucas Beyer. 2023. [Sigmoid loss for language image pre-training](#). In *Proceedings of the IEEE/CVF International Conference on Computer Vision (ICCV)*, pages 11975–11986.
- Yanzhe Zhang, Ruiyi Zhang, Jiuxiang Gu, Yufan Zhou, Nedim Lipka, Diyi Yang, and Tong Sun. 2023. [Llavar: Enhanced visual instruction tuning for text-rich image understanding](#). *Preprint*, arXiv:2306.17107.
- Lianmin Zheng, Wei-Lin Chiang, Ying Sheng, Siyuan Zhuang, Zhonghao Wu, Yonghao Zhuang, Zi Lin, Zhuohan Li, Dacheng Li, Eric Xing, Hao Zhang, Joseph E. Gonzalez, and Ion Stoica. 2023a. [Judging LLM-as-a-judge with MT-bench and chatbot arena](#). In *Thirty-seventh Conference on Neural Information Processing Systems Datasets and Benchmarks Track*.
- Lianmin Zheng, Liangsheng Yin, Zhiqiang Xie, Jeff Huang, Chuyue Sun, Cody Hao Yu, Shiyi Cao, Christos Kozyrakis, Ion Stoica, Joseph E. Gonzalez, Clark Barrett, and Ying Sheng. 2023b. [Efficiently programming large language models using sglang](#). *Preprint*, arXiv:2312.07104.
- Álysson Soares, Ricardo das Neves Junior, and Byron Bezerra. 2020. [Bid dataset: a challenge dataset for document processing tasks](#). In *Anais Estendidos do XXXIII Conference on Graphics, Patterns and Images*, pages 143–146, Porto Alegre, RS, Brasil. SBC.
- ## A Analysis on Model Training Cost and Comparison to Other Models
- Table 7 delivers a comprehensive analysis of the training costs incurred with different model sizes of ELVA, utilizing 8 A100 GPUs. As per estimates drawn from the official blog of LLaVA-NeXT<sup>3</sup>, the training times of our models are roughly 1.38 to 1.8 times longer. They reported requiring 20 hours to train a 7B model with 8 A100 GPUs, and 24 hours for a 13B model using 16 A100 GPUs. Although the precise training time may vary based on the testing environment, our data suggests that ELVA’s training costs comparable.
- The comparison is more evident when juxtaposed with contemporary, data-intensive models like QwenVL (Bai et al., 2024), which calls for 1.4B data points for pretraining and 50M for instruction tuning. Given concerns about increased data and resources, our model offers a different perspective. For instance, compared to QwenVL’s significant resource investment, ELVA approach exhibits modest yet effective resource use.
- Models like Shikra (Chen et al., 2023a), Idefics2 (Laurençon et al., 2024) and InternLM-XComposer2-4KHD (Dong et al., 2024), illustrate various scales of resource utilization. Shikra utilizes 600K data points for alignment and 5.5M for instruction tuning, Idefics2 reveals impressive outcomes with over 1B data points, and InternLM-XComposer2-4KHD demonstrates the ability to scale up with a massive volume of training data and more than 8,000 input tokens.
- Our observations in Section 4.3 further reinforce the argument for ELVA’s efficiency. Despite additional data, LLaVA-1.5 failed to surpass the overall score we achieved with ELVA (C5 vs. C6), further substantiating the efficiency and effectiveness of ELVA. Furthermore, it is essential to accentuate the inference cost’s importance. Models aiming for reduced inference costs often encounter expensive training costs and challenges in maintaining instruction-following capabilities across varied response lengths (Dai et al., 2023; Liu et al., 2023b; Laurençon et al., 2024). Thus, ELVA presents as a quick, lightweight, and cost-effective alternative within LLaVA-like simple architectures.
- Moreover, we observe ongoing initiatives to develop compact yet robust VLMs within the range of 1B to 3B parameters (Chu et al., 2024). These

<sup>3</sup><https://llava-v1.github.io/blog/2024-01-30-llava-next>



Model Size	Alignment Time	Instruct Tuning Time	Total Time
0.2B	0.5 hours	3 hours	3.5 hours
1B	1.5 hours	6 hours	7.5 hours
3.8B	4.5 hours	18.5 hours	23 hours
7B	6.5 hours	29.5 hours	36 hours
13B	11 hours	55 hours	66 hours

Table 7: Training times for various model sizes on 8 A100 GPUs.

Dataset	# Samples
LLaVA	157,712
SG40k	40,688
VQA-v2	82,783
GQA	72,140
OKVQA	8,998
OCRQA	80,000
A-OKVQA	66,160
TextCaps	21,953
RefCOCO	48,447
VG	86,417

Table 8: Dataset proportions for LLaVA-1.5 (Liu et al., 2023b). RefCOCO and VG were not used in ELVA ablation studies.

works predominantly concentrate on general image processing. Remarkably, effective VLMs explicitly designed for visually-situated NLU tasks, like processing high-resolution document images, are still limited, highlighting our work’s primary focus.

## B Implementation Details

### B.1 Software and Hardware Setup

Our experiments are performed using the official code of LLaVA (Liu et al., 2023c)<sup>4</sup>. We utilize NVIDIA V100 and A100 GPUs for the computations. Ablation studies are conducted on V100 GPUs, whereas the final configuration models run on A100 GPUs. We do not observe any significant performance difference based on the type of GPU used. However, training on V100 GPUs is approximately 2 to 3 times slower per step compared to A100 GPUs. Although our codebase is based on LLaVA, to ensure better reproducibility, we will release the scripts used for training our models and any necessary code modifications as open-source.

### B.2 Datasets and Hyperparameters

**Initial Curated Dataset from LLaVA-1.5.** Table 8 provides detailed quantities of the subsets within the dataset.

**Datasets.** Table 9 lists the datasets in Elva’s final configuration. Meanwhile, for the alignment phase,

<sup>4</sup><https://github.com/haotian-liu/LLaVA>

Dataset	# Samples	Sampling Ratio %
LLaVA-1.5-Set (Liu et al., 2023b) (See Table 8)	665,298	46.49
Vision-Flan-Set (Xu et al., 2024)	186,103	12.99
WikiArt (Chen et al., 2023b)	500	0.03
Celebrity (Chen et al., 2023b)	498	0.03
Landmark (Chen et al., 2023b)	500	0.03
Share-TextVQA (Chen et al., 2023b)	500	0.03
DocVQA (Mathew et al., 2021)	11,480	1.60
ChartQA (Masry et al., 2022)	18,317	2.56
*Cauldron-Set-AI2D	2,434	0.17
*Cauldron-Set-Chart2Text	26,961	1.88
*Cauldron-Set-Diagram-Image-to-Text	300	0.02
*Cauldron-Set-HITAB	2,500	0.17
*Cauldron-Set-IAM	5,663	0.40
*Cauldron-Set-RenderedText	10,000	0.70
*Cauldron-Set-Robot-SQA	8,514	0.59
*Cauldron-Set-Robot-WTQ	38,246	2.67
*Cauldron-Set-ScienceQA	4,976	0.35
*Cauldron-Set-Screen2words	15,730	1.10
*Cauldron-Set-STVQA	17,247	1.20
*Cauldron-Set-TabMWP	22,722	1.59
*Cauldron-Set-InfoVQA	2,118	0.15
*Cauldron-Set-TQA	1,493	0.10
CORD-Instruct (Proposed in this work, §5.2)	680	0.05
VisualMRC (Tanaka et al., 2021)	7,959	0.56
LLaVAR-Inst (Zhang et al., 2023)	19,732	1.38
DocReason (Hu et al., 2024)	25,877	1.81
DocVQA-single <sup>†</sup>	44,815	9.38
ChartQA-single <sup>†</sup>	28,068	5.88
Layout-en-sampled <sup>‡</sup> (Kim et al., 2023)	50,000	3.49
DVQA-sampled <sup>‡</sup> (Kaffe et al., 2018)	10,000	0.70
MMC-Chart-sampled <sup>‡</sup> (Liu et al., 2024a)	10,000	0.70
ScreenQA-sampled <sup>‡</sup> (Hsiao et al., 2024)	10,000	0.70
LRV-Chart-sampled <sup>‡</sup> (Liu et al., 2023a)	6,746	0.47

Table 9: Overview of datasets used in ELVA’s final data configuration. All datasets are open-source and freely accessible. Datasets marked with \* are subsets curated by Laurençon et al. (2024), with only selected portions adopted in this work. <sup>†</sup> indicates that each question-answer pair is considered as a single sample. Datasets marked with <sup>‡</sup> had a large volume of data, hence, only partial images were randomly sampled.

we used the respective alignment datasets from LLaVA (Liu et al., 2023c) and LLaVAR (Zhang et al., 2023), which consist of 558K and 422K samples respectively.

**Hyperparameters.** Table 10 and Table 11 outline the hyperparameters applied during the alignment and instruction tuning stages, noting that smaller models thrive with larger learning rates. In the final model training configuration, we use the data and sampling ratios from Table 9 and train the model for 11K steps. The exact number of unique images is difficult to calculate since some images are shared across datasets, but we estimate using approximately 1M unique images. Note that LLaVA-NeXT reported using 760K samples,<sup>5</sup> indicating a modest increase in our case. Moreover, as we leverage multiple curated datasets with slightly different questions on the same images, we consider a synthetic epoch to consist of 1.4M examples. Thus, with a batch size of 128, we run 11K steps

<sup>5</sup><https://llava-v1.github.io/blog/2024-01-30-llava-next>

Model Size	LR	Epsilon	Grad Clip Norm	Weight Decay	Warmup Ratio
0.2B	1e-3	1e-6	0.5	0.0	0.03
1B	1e-3	1e-6	0.5	0.0	0.03
3.8B	1e-3	1e-6	0.5	0.0	0.03
7B	1e-4	1e-6	0.5	0.0	0.03
13B	1e-4	1e-6	0.5	0.0	0.03

Table 10: Hyperparameters used during the alignment stage.

Model Size	LR	Epsilon	Grad Clip Norm	Weight Decay	Warmup Ratio
0.2B	3e-4	1e-6	0.5	1e-3	0.03
1B	3e-4	1e-6	0.5	1e-3	0.03
3.8B	2e-4	1e-6	1.0	0.0	0.03
7B	2e-5	1e-6	1.0	0.0	0.03
13B	2e-5	1e-6	1.0	0.0	0.03

Table 11: Hyperparameters used during the instruct tuning stage. Larger learning rates were noted to be more effective for smaller models.

(1.4M / 128). For the Ablation studies, we exclude datasets like VG, RefCOCO, and Vision-Flan to reduce the cost, resulting in 9K training steps. Additionally, the 0.2B model converges more slowly, so we run this model for twice the number of steps compared to the other models (1B to 13B). This increased number of steps is applied only to the 0.2B model.

## C Details on the Construction of the Newly Generated Datasets

### C.1 CORD-Instruct

CORD (Park et al., 2019) provides Indonesian receipt data along with structured information represented in JSON format. Our goal was to generate a dataset that requires models to produce outputs in specific formats such as JSON, XML, or Markdown.

The CORD-Instruct dataset is generated using the OpenAI GPT-3.5 API. A detailed prompt is crafted (as outlined in Table 13) to guide the API in generating synthetic user queries and corresponding responses based on the given structured information.

After generating initial instructions and OpenAI’s response with synthetic questions and answers, we manually filtered and annotated the samples to ensure they accurately represented real-world scenarios. This includes removing ambiguous instructions and correcting poorly transcribed JSON, XML, or Markdown outputs.

### C.2 Parsing-Bench

Parsing-Bench is a dataset tailored to meet the practical needs of document assistants. In-

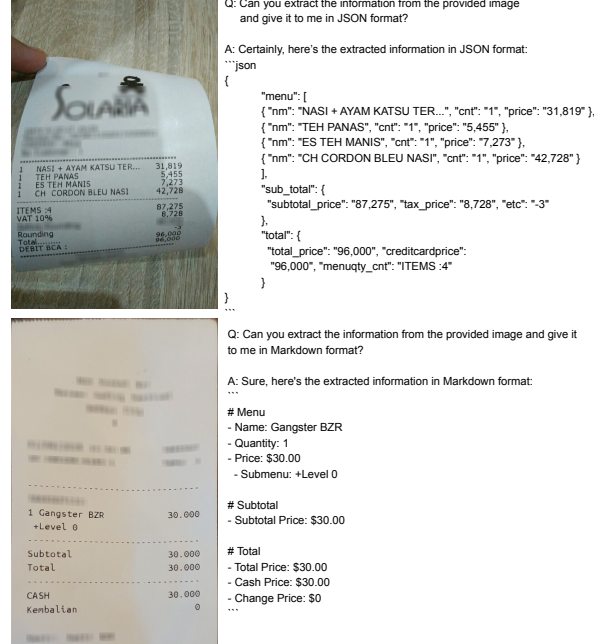


Figure 7: The generated examples of CORD-Instruct.

spired by LLaVA-Bench, it includes tasks that require careful interpretation and analysis of documents. We incorporate Brazilian Identity Documents (BID) (Álysson Soares et al., 2020) and SROIE (Huang et al., 2019) in its creation. Tables 15 and Tables 16 show the prompts we use to extract information from images.

The evaluation process is visually depicted in Figure 8 for a better understanding of our method. Parsing-Bench includes examples that necessitate the model to extract and interpret information from diverse documents. These instances have been specifically designed to test the models’ understanding and reasoning skills.

As part of our commitment to sharing our research output for the benefit of others, the datasets will be made publicly available.

## D ELVA-encoder Training

**Training Details.** As explained in Section 4.3, each *REncoder* variant is trained by unfreezing the vision encoder and fine-tuning it on a minimal VLM (1B scale) with text-centric datasets. We opt for a 1B parameter model to strike a balance between computational requirements and model performance. A larger model might further enhance text recognition, but it significantly increases computational needs and training time. The previous attempt with a 160M-parameter model worked but showed room for improvement in terms of perfor-

Batch Size	Learning Rate (LR)	Weight Decay
128	5e-5	1e-3
128	6e-5	1e-3
128	7e-5	1e-3
128	8e-5	1e-3
256	5e-5	1e-3
256	6e-5	1e-3
256	7e-5	1e-3
256	8e-5	1e-3
512	5e-5	0.0
512	6e-5	0.0
512	7e-5	0.0
512	8e-5	0.0

Table 12: The configurations for 12 difference *REncoder* training, including batch size, learning rate, and weight decay. Other hyperparameters basically identical to §B.2.

mance. Consequently, a 1B parameter model was selected for substantial enhancements, yet affording efficiency in computational resource use.

Our training procedure mainly focuses on text reading tasks to fortify the vision encoder’s text recognition abilities. The training datasets are OCR-IDL (Biten et al., 2022) (837,922 samples utilized), PDFa<sup>6</sup> (1,048,569 samples utilized), LLaVA (Liu et al., 2023c) alignment set, and LLaVAR (Zhang et al., 2023) alignment set. We allow duplicate sampling, treating 3.5M samples as a virtual epoch, and perform 1 epoch of training with the configuration depicted in Table 12. This procedure is repeated creating 12 distinct variants of the REncoder. The chosen model scale supports rapid iterations, with each session taking roughly 1.7 days using 8 V100 GPUs.

**Weight Averaging with Model Soup.** Although Wortsman et al. (2022) proposed a greedy soup method involving validation where some models are averaged or rejected, we employed a uniform averaging technique referred to as “uniform soup” in the paper.

## E Prompts used in RR Prompts

As seen in Table 14, we insert a preliminary QA turn where the model is prompted to read the text in the image using simple commands. Although the idea is straightforward, we observe that it leads to better training outcomes for the model. To avoid specialization to a single OCR engine, we use a

<sup>6</sup><https://huggingface.co/datasets/pixparse/pdfa-eng-wds>

### CORD-Instruct Generation Prompt

Create a synthetic user query requesting information extraction from a given document image. The extracted information should be provided in various formats such as JSON, XML, or Markdown based on the user’s request. Users may ask for specific parts of the information, like menu items or payment amounts. Your task is to generate both a user query and the corresponding response from the information extraction system. Ensure the queries and responses vary in detail and format. Sometimes include concise responses, particularly when indicated with the word “concisely.”

The provided JSON is to guide your response creation - do not display or mention it in the user queries. Specifically, do not create queries that ask for information extraction from a provided JSON (e.g., “Can you extract the information from the provided JSON” is not allowed). Additionally, you do not need to strictly follow the tag names in the provided JSON while creating your responses (e.g., “nm” can be “name” or “cnt” can be “count”). Return results strictly in the format shown below:

```
Query: I need the payment amount
from the document in this image
in JSON format, answer concisely.
Answer: <<<json
{
  "payment_amount": "$123.45"
}
>>>
```

```
Query: Please parse the input document
and provide the menu details in XML.
Answer: Certainly, here is the menu
information in XML format:...
```

```
Query: Can you provide the extracted
customer information from the document
image in Markdown?
Answer: Sure, here it is:
<<<
# Customer Information
- Name: John Doe
- Email: john.doe@example.com
>>>
```

Remember, the goal is to include appropriate formatting such as JSON, XML, or Markdown in your responses to correspond with the user’s query.

Table 13: CORD-Instruct Prompt for Data Generation.

mix of MS OCR<sup>7</sup> and CLOVA OCR<sup>8</sup> annotations. In text-heavy samples like those in DocVQA, the CLOVA OCR API takes approximately 4 seconds per call. However, we believe this cost can be optimized in future iterations.

<sup>7</sup><https://docs.microsoft.com/en-us/azure/cognitive-services/computer-vision/overview-ocr>.

<sup>8</sup><https://clova.ai/ocr/en>

Prompt
Carefully decipher the text in this image. Provide the text in the image only.
Investigate the image for any text. Provide the text in the image only.
Examine the image for any letters or words. Provide the text in the image only.
Identify all written characters present in the image. Provide the text in the image only.
Do a careful reading of the image and transcribe all text. Provide the text in the image only.
Inspect the image and write down all readable characters. Provide the text in the image only.
Translate the image content into written text. Provide the text in the image only.
Review the image and offer a transcription of the text. Provide the text in the image only.
Look over the image and jot down all visible text. Provide the text in the image only.
Scrutinize the image for any discernible words or letters. Provide the text in the image only.
Study the image and document all characters found within. Provide the text in the image only.
Assess the image and record any visible words or letters. Provide the text in the image only.
Kindly extract any text or characters from this image. Provide the text in the image only.
Evaluate the image and isolate all written content. Provide the text in the image only.
Assimilate all readable characters within the image. Provide the text in the image only.
Decode any legible text visible in the image. Provide the text in the image only.
Grasp all written elements within the image. Provide the text in the image only.
Conduct a thorough examination of the image and capture all text. Provide the text in the image only.
Peel all readable characters out from the image. Provide the text in the image only.
Interpret all characters from the image. Provide the text in the image only.
Understand and transcribe any textual content from the image. Provide the text in the image only.
Dissect the image and recover any written characters. Provide the text in the image only.
Deduce and present all visible text from the image. Provide the text in the image only.
Inspect the image and translate any visible characters into text. Provide the text in the image only.

Table 14: Prompt examples for text reading tasks used in Read-and-Reason Prompting.

**BID Context Generation Prompt**

Using the provided Brazilian Identity Document image, please compose a comprehensive and detailed caption that encapsulates all the elements depicted in the image. Ensure precision in extracting any text present, maintaining case sensitivity and retaining the exact original form. Begin with a well-written caption in natural language, detailing the image’s content, layout, and nuances. Conclude with a well-structured XML format that meticulously documents the extracted information, preserving the image’s original layout and details.

Table 15: Parsing-Bench Context Generation Prompt for BID Dataset (Állysson Soares et al., 2020).

**SROIE Context Generation Prompt**

Using the provided scanned receipt image, please compose a comprehensive and detailed caption that encapsulates all the elements depicted in the image. Ensure precision in extracting any text present, maintaining case sensitivity and retaining the exact original form. Begin with a well-written caption in natural language, detailing the image’s content, layout, and nuances. Conclude with a well-structured XML format that meticulously documents the extracted information, preserving the image’s original layout and details.

Table 16: Parsing-Bench Context Generation Prompt for SROIE Dataset (Huang et al., 2019).



Can you summarize the purchased item information, including the name, price, and quantity, in XML format?



Certainly, here is the purchased item information in XML format:

```

'''xml
<purchased_items>
  <item>
    <name>GREEN TEA</name>
    <quantity>1</quantity>
    <price>3.00</price>
  </item>
  <item>
    <name>GREEN TEA</name>
    <quantity>1</quantity>
    <price>3.00</price>
  </item>
  <item>
    <name>BUFFET DINNER (ADULT)</name>
    <quantity>3</quantity>
    <price>49.90</price>
  </item>
</purchased_items>
'''
ELva received 9/10

```

REVIEW:  
8 9

Assistant 1 provided a clear and accurate summary of the purchased items in XML format. However, the XML tags used ("Receipt", "Item", "Name", "Price", "Quantity") are not consistent with the tags used in the original XML provided by the user. This inconsistency might cause confusion or require additional work to integrate with the user's existing data structure.

Assistant 2 also provided a clear and accurate summary of the purchased items in XML format. The tags used ("purchased\_items", "item", "name", "quantity", "price") are more consistent with the original XML structure provided by the user, making it easier to integrate and more relevant. Additionally, Assistant 2's response includes a root tag ("purchased\_items") that encapsulates all items, which is a good practice for XML structure.

Overall, both assistants performed well, but Assistant 2's response is slightly more aligned with the user's existing data structure and includes better XML formatting practices.

The image is a scanned receipt from ROCKU YAKINIKU, a restaurant located at CPI ROCKU SDN. BHD. (1096317-P), LOT F355/356/357, FIRST FLOOR, RAINFOREST, 1 UTAMA SHOPPING CENTRE, LEBUH BANDAR UTAMA, 47800 PETALING JAYA. The receipt includes the GST number 000446271488. The transaction took place on 19/02/2018 at 17:43, with the cashier identified as CASHIER and the server as BISWASH(ip). The table number is A9, and there were 3 people (Pax: 3). The bill number is 063975.

The items ordered include:

- 1 Green Tea at RM 3.00
- 1 Green Tea at RM 3.00
- 3 Buffet Dinner (Adult) at RM 49.90 each, totaling RM 149.70

The subtotal is RM 155.70. Additional charges include a 10% service charge of RM 15.57 and a 6% GST of RM 10.28, bringing the total to RM 181.55. The payment was made in cash, with RM 201.55 given, resulting in a change of RM 20.00.

The GST Summary shows:

- T: 6% GST on an amount of RM 171.27, with a tax of RM 10.28
- Z: Zero Rated with an amount of RM 0.00 and a tax of RM 0.00

The receipt concludes with a space for a signature and a thank you note, "Thank you. Please come again." The bill was closed at 19:08:04.

```

'''xml
<receipt>
  <restaurant>
    <name>ROCKU YAKINIKU</name><company>CPI ROCKU SDN. BHD. (1096317-P)</company><gst_no>000446271488</gst_no>
    <address><lot>LOT F355/356/357, FIRST FLOOR</lot><location>RAINFOREST, 1 UTAMA SHOPPING CENTRE</location><street>LEBUH
    BANDAR UTAMA</street><city>47800 PETALING JAYA</city></address>
  </restaurant>
  <transaction>
    <date>19/02/2018</date><time>17:43</time><terminal>T001</terminal><bill_no>A063975</bill_no>
    <cashier>CASHIER</cashier><server>BISWASH(ip)</server><table>A9</table><pax>3</pax><bill>063975</bill>
  </transaction>
  <items>
    <item><name>GREEN TEA</name><quantity>1</quantity><price>3.00</price><total>3.00</total><tax>T</tax></item>
    <item><name>GREEN TEA</name><quantity>1</quantity><price>3.00</price><total>3.00</total><tax>T</tax></item>
    <item><name>BUFFET DINNER (ADULT)</name><quantity>3</quantity><price>49.90</price><total>149.70</total><tax>T</tax></item>
  </items>
  <summary><subtotal>155.70</subtotal><service_charge>15.57</service_charge><gst>10.28</gst><total>181.55</total>
  <payment><method>CASH</method><amount>201.55</amount><change>20.00</change></payment>
</summary>
<gst_summary>
  <gst><type>T</type><rate>6%</rate><amount>171.27</amount><tax>10.28</tax></gst>
  <gst><type>Z</type><rate>Zero Rated</rate><amount>0.00</amount><tax>0.00</tax></gst>
</gst_summary>
<footer>
  <signature>_____</signature><note>Thank you. Please come again</note><bill_close>19:08:04</bill_close>
</footer>
</receipt>
'''

```

Figure 8: The top left displays the question and the model prediction results. The top right contains the received review. The bottom part, as introduced in Section C.2, exhibits the image's context prepared through prompting. The evaluation compares two model predictions by inputting them into a high-performance LLM along with this context. In this example review, ELVA is assistant 2.